Theor Chim Acta (1995) 92: 199–210

Theoretica
Chimica Acta

A theoretical study on the ionization of furan with analysis of vibrational structure of the photoelectron spectra

Kouichi Takeshita[1], **Yuichi Yamamoto**[2]

[1] Faculty of Bioindustry, Tokyo University of Agriculture, Abashiri, Hokkaido 099-24, Japan

[2] The Center for Information Processing Education of Hokkaido University, Sapporo 060, Japan

Received June 7, 1994/Accepted February 27, 1995

Summary. *Ab initio* calculations have been performed to study on the molecular structures and the vibrational levels of the low-lying ionic states ($^2A_2$ and $^2B_1$) of furan. The equilibrium molecular structures and vibrational modes of these states are presented. The theoretical ionization intensity curves including the vibrational structures of the low-lying two ionic states are also presented and compared with the photoelectron spectrum. A number of new assignments of the photoelectron spectra are proposed.

Key words: Furan cation – RHF/gradiend – Molecular-structure vibrationally-analysis – Franck–Condon-factor PE-spectrum

1. Introduction

The electronic configuration of the ground state of furan is represented by a ... $(5b_2)^2\,(1b_1)^2\,(6b_2)^2\,(8a_1)^2\,(9a_1)^2\,(2b_1)\,^2(1a_2)^2$. The photoelectron (PE) spectroscopy investigations of furan have been reported by many workers [1–7]. The assignment of the electronic states of the lowest two bands was established. The lowest state was the $^2A_2$ state and the second was the $^2B_1$ state. These states show well-resolved vibrational structures. The assignment of the vibrational levels was attempted by Derrick et al. [3]. They interpreted the vibrational structure by taking into account the vibrational modes and frequencies of the ground state.

The theoretical approaches on furan have been reported [8–11]. Many workers have calculated the vertical ionization energies in order to help the assignment of the electronic states of the PE spectra.

As a molecule is ionized, the equilibrium molecular structure and the character of the vibrational mode should change from those of the ground state. The vibrational structure of the PE spectrum reflects these changes. It is, therefore, interesting to investigate the vibrational structure associated with the change in the equilibrium molecular structure and the vibrational mode by ionization.

No theoretical investigation on the molecular structures and the vibrational levels of the ionic states has been reported. In this work, we determine the equilibrium molecular structures of the ground and lower ionic states by using the *ab initio* self-consistent-field (SCF) method. Within the framework of the adiabatic approximation and the harmonic oscillator approximation, we calculate the harmonic force constant matrix elements over variables of the totally symmetric distortion and the vibrational frequencies of the totally symmetric modes. We obtain approximate theoretical intensity curves using the Franck–Condon factor (FCF) which is given by the square of the overlap integrals between the vibrational wave function of the ground state and that of the ionic state. Based on these calculations, we discuss the vibrational levels of the low-lying ionic states compared to the photoelectron spectrum.

2. Method of calculations

We used the basis sets of the MIDI-4-type prepared by Tatewaki and Huzinaga [12]. These were augmented by one p-type polarization function for H and one d-type polarization function for C and O. The exponents of the polarization function for H, C and O are 0.68, 0.61 and 1.16, respectively.

The gradient technique for the Roothaan's restricted Hartree–Fock (RHF) method was used to determine the optimum molecular structures of the ground state and the ionic states.

The single- and double-excitation configuration interaction (SDCI) method was used to obtain more accurate ionization energies for the estimation of a vertical ionization energy (VIE) and adiabatic ionization energy (AIE). A single reference configuration of an SCF wave function of the respective state was used. In the SDCI method, singly and doubly excited configuration state functions (CSFs) were generated where the inner shells were kept frozen. The generated CSFs were then restricted to the first-order interacting space [13]. Since the dimensions of the CI were too large, we adopted a CSF selection process by the use of second-order perturbation theory. The threshold for the selection was 8 μHartree. The number of the generated CSFs were reduced from about 120000 to 16000. We estimated the total energy including the contribution from the rejected CSFs by a second-order perturbation theory [14].

The harmonic force constant matrix elements were calculated by means of the gradient technique with the RHF wave function; the second derivative was estimated by the numerical differentiation of the analytically calculated first derivative. We calculated the FCFs of only the totally symmetric vibrational modes. In calculating FCFs, we approximated the vibrational wave functions by those obtained by the harmonic oscillator model. We assumed that the initial state was the zero point vibrational level of the ground state. The method of calculation of the FCF and theoretical intensity curves was the same as we used in the previous paper [15].

This work was carried out by using the computer program system GRAMOL [16] for the gradient technique and the calculation of normal modes, and MICA3 [17] for the CI calculations.

3. Results and discussion

Table 1 shows the optimized geometrical parameters of the ground and ionic states. A numbering of each atom is illustrated in Fig. 1. The optimized geometric parameters of the ground state are in good agreement with the experimental ones

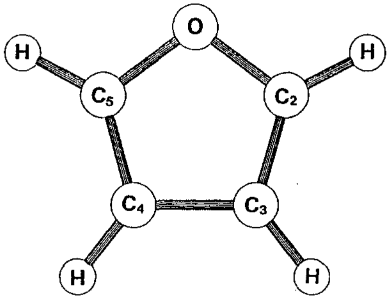

Fig. 1. A numbering of each atom

[18]. Table 1 also shows a magnitude of the change in the equilibrium molecular structure by ionization.

Table 2 shows the VIE and AIE at the SCF and SDCI levels. In the SDCI calculations, the weights of the reference function of the $^1A_1$, $^2A_2$ and $^2B_1$ states at the optimized geometry are 86.3%, 86.7% and 86.1%, respectively. The table also shows the energy lowering of the AIE compared to the VIE. The energy lowering of the $^2A_2$ and $^2B_1$ states at the SDCI level are 0.30 and 0.49 eV, respectively.

The 0–0 ionization energies at the SDCI level and the FCFs of the 0–0 transitions are listed in Table 2. The FCFs of the $^2A_2$ and $^2B_1$ states are so large that the 0–0 transitions should be observed. Derrick et al. reported that the observed 0–0 bands of the $^2A_2$ and $^2B_1$ states were 8.9 and 10.3 eV, respectively. The present calculated values are underestimated by 0.66 and 0.43 eV in comparison with the observed values.

The vibrational frequencies of the ground and ionic states are shown in Table 3. The frequencies are arranged in order of magnitude. Comparing with the observed values [19] of the $^1A_1$ state, we overestimate the frequencies by 9.1–12.7% except for the ν_8 mode. The frequency of the ν_8 mode is overestimated by 31.9%. However, Derrick et al. proposed that the frequency of the ν_8 mode should be 839 cm^{-1}. Comparing with this value, we overestimate by 13.8%. Each mode is characterized by a conventional potential energy distribution (PED) and a classical half-amplitude of the zero-point vibrational levels. Table 4 shows the PED which is described using the totally symmetrical displacement coordinate. The classical half-amplitude is shown in Table 5.

For the interpretation of each mode of the $^1A_1$ state, Table 4 shows that the ΔS_3 and ΔS_4, totally symmetrical displacement coordinates, contribute mainly to the PED of the ν_1 and ν_2 modes, respectively. The ΔS_3 and ΔS_4 coordinates are connected to the C_2–H (and C_5–H) and C_3–H (and C_4–H) stretching motions, respectively. Thus, the ν_1 and ν_2 modes should be interpreted as the C_2–H and C_3–H stretching motions, respectively. Table 4 indicates that the ΔS_1 coordinate contributes to the ν_6 mode. The ΔS_1 coordinate describes the O–C_2 (and O–C_5) stretching motion. Therefore, the character of the ν_6 mode is the O–C stretching motion. The ν_8 mode is a mixture of the ΔS_5 and ΔS_6 coordinates. The symmetrical displacement coordinates of the ΔS_5 and ΔS_6 are C_2–O–C_5 and O–C_2–C_3 (and O–C_5–C_4) bending motions, respectively. It is evident from Table 5 that the two motions couple with out-of-phase. Therefore, the ν_8 mode is a mixture of the C–O–C and O–C–C bending motions coupled with out-of-phase mode. We are not able to make clear-cut interpretations of the ν_3, ν_4, ν_5 and ν_7 modes. The ΔS_1, ΔS_2,

Table 1. Optimized molecular structure and magnitude of the change in the geometry by ionization

State	O–C$_2$ (ΔO–C$_2$)	C$_2$–C$_3$ (ΔC$_2$–C$_3$)	C$_3$–H(ΔC$_2$–H)	C$_3$–H(ΔC$_3$–H)
$^1A_1$	1.342	1.343	1.076	1.078
Exp.[a]	1.362	1.361	1.075	1.077
$^2A_2$	1.321(− 0.020)	1.404(+ 0.061)	1.080(+ 0.004)	1.079(+ 0.001)
$^2B_1$	1.316(− 0.026)	1.366(+ 0.023)	1.076(+ 0.000)	1.080(+ 0.002)
State	C$_2$–O–C$_5$ (ΔC$_2$–O–C$_5$)	O–C$_2$–C$_3$ (ΔO–C$_2$–C$_3$)	O–C$_2$–H (ΔO–C$_2$–H)	C$_2$–C$_3$–H (ΔC$_2$–C$_3$–H)
1A$_1$	107.30	110.83	116.33	126.65
Exp.[a]	106.6	110.7	115.9	126.1
$^2A_2$	107.57(+ 0.27)	110.54(− 0.29)	117.18(+ 0.85)	125.49 (− 1.16)
$^2B_1$	113.56 (+ 6.26)	108.54 (− 2.29)	117.83 (+ 1.50)	128.20 (+ 1.55)

[a] Ref. [18]

Bond lengths are in angstroms, angles in degrees

The values in parenthesis are the magnitude of the change in geometry by ionization

Table 2. Ionization energies (eV)

State	VIE		AIE		Δ(VIE − AIE)		0–0 transition	
	SCF	SDCI	SCF	SDCI	SCF	SDCI	0–0 IE	FCF
$^2A_2$	7.88	8.53	7.60	8.23	0.28	0.30	8.24	0.211
$^2B_1$	10.03	10.37	9.51	9.88	0.52	0.49	9.87	0.205

VIE: Vertical ionization energy. AIE: Adiabatic ionization energy
0–0 IE: 0–0 ionization energy at the SDCI level. FCF: Franck–Condon factor
Total energies (a.u.) of $^1A_1$: −228.3753081 (SCF) and −229.001064 (SDCI)

Table 3. Vibrational frequencies (cm^{-1})

State	ν_1	ν_2	ν_3	ν_4	ν_5	ν_6	ν_7	ν_8
$^1A_1$	3456	3421	1671	1537	1249	1160	1076	955
Obs.[a]	3121	3089	1483	1380	1138	1061	986	724
$^2A_2$	3448	3432	1659	1578	1265	1187	1146	953
$^2B_1$	3472	3431	1589	1498	1222	1185	1026	935

[a] Ref. [19].

ΔS_5, ΔS_6, ΔS_7, and ΔS_8 coordinates contribute to these modes, while the contributions of the ΔS_3 and ΔS_4 coordinates are negligibly small.

The characters of the ν_1 and ν_2 modes of the $^2A_2$ and $^2B_1$ states are the same as those of the $^1A_1$ state. However, in the $^2A_2$ state, the coupling of the C_2–H and C_3–H stretching motions becomes more strong, while the coupling becomes more weak for the $^2B_1$ state. It is evident from Tables 4 and 5 that the characters of the ν_8 modes of the $^2A_2$ and $^2B_1$ states correspond to that of the ν_8 mode of the $^1A_1$ state. It is also evident from Tables 4 and 5 that the characters of the ν_3, ν_4 and ν_6 modes of the $^2B_1$ state are almost the same as those of the ground state. Table 5 reveals that characters of the ν_5 and ν_7 modes of $^2B_1$ correspond to those of $^1A_1$. Therefore, the characters of all modes of the $^2B_1$ state should correspond to those of the ground state. Table 5 also shows that the character of the ν_7 mode of $^2A_2$ corresponds to that of the ν_7 mode of $^1A_1$. It also indicates that the character of the ν_4 mode of the $^2A_2$ state should correspond to that of the ν_3 mode of the ground except for the amplitude of the C_2–C_3–H bending motion. However, for the ν_3, ν_5 and ν_6 modes of the $^2A_2$ state, we are not able to find any correspondence with the vibrational modes of the ground state.

The theoretical intensity curves of the $^2A_2$ and $^2B_1$ states are illustrated in Fig. 2 by assuming a half-width of 0.08 eV for each transition band. It is compared with the observed PE spectrum by Turner et al. [2]. The theoretical intensity curve imitates well the vibrational structure of the observed PE spectrum. In order to discuss more detailed vibrational structure of each band, we illustrate the theoretical intensity curve with a half-width of 0.02 eV. The result is shown in Figs. 3 and 4. The assignment of the vibrational structures of the $^2A_2$ and $^2B_1$ states are found in Tables 6 and 7, respectively.

Table 6 shows the vibrational energy, intensity and assignment of each vibrational level appearing in Fig. 3. The vibrational levels of FCF values larger than

Table 4. Conventional potential energy distribution (%)

State	Component	ν_1	ν_2	ν_3	ν_4	ν_5	ν_6	ν_7	ν_8
$^1A_1$	ΔS_1	0.3	0.1	9.2	12.1	7.0	82.6	18.8	0.4
	ΔS_2	1.0	0.1	27.3	8.6	16.0	0.8	0.2	0.0
	ΔS_3	79.7	15.5	0.1	0.1	0.1	0.1	0.0	0.0
	ΔS_4	14.6	81.6	0.2	0.0	0.3	0.1	0.1	0.0
	ΔS_5	2.6	0.3	40.9	0.6	4.4	1.4	31.8	55.3
	ΔS_6	1.8	2.3	8.2	47.7	25.9	6.1	12.7	43.4
	ΔS_7	0.1	0.0	14.2	6.8	31.7	8.0	2.7	0.0
	ΔS_8	0.0	0.1	0.1	24.1	14.8	1.0	33.8	0.8
$^2A_2$	ΔS_1	0.3	0.2	25.2	6.5	62.1	18.2	30.8	0.2
	ΔS_2	0.8	0.0	0.5	12.6	13.3	30.8	0.8	0.1
	ΔS_3	65.5	28.9	0.0	0.1	0.5	0.0	0.0	0.0
	ΔS_4	28.8	64.9	0.3	0.0	0.4	0.1	0.0	0.0
	ΔS_5	3.0	1.1	20.4	38.3	7.8	10.9	30.0	52.9
	ΔS_6	1.6	4.8	23.2	30.5	12.1	4.9	1.9	46.3
	ΔS_7	0.1	0.0	15.6	9.2	0.0	29.9	1.7	0.0
	ΔS_8	0.0	0.1	14.8	2.9	3.7	5.3	34.7	0.4
$^2B_1$	ΔS_1	0.4	0.0	11.1	12.9	23.8	65.1	3.7	0.0
	ΔS_2	0.8	0.2	19.7	11.7	20.5	4.4	0.0	0.2
	ΔS_3	87.5	7.4	0.1	0.2	0.2	0.1	0.0	0.0
	ΔS_4	6.9	90.7	0.1	0.0	0.4	0.0	0.3	0.0
	ΔS_5	2.2	0.1	40.9	1.9	4.0	8.3	2.1	56.2
	ΔS_6	2.1	1.5	9.5	41.7	11.9	3.5	67.8	43.0
	ΔS_7	0.1	0.0	18.7	5.8	10.8	16.8	3.3	0.0
	ΔS_8	0.0	0.1	0.1	25.7	28.4	1.8	22.8	0.5

The definitions of the totally symmetrical displacement coordinates are as follows:

$\Delta S_1 = (\Delta O\text{–}C_2 + \Delta O\text{–}C_5)/\sqrt{2}$

$\Delta S_2 = (\Delta C_2\text{–}C_3 + \Delta C_5\text{–}C_4)/\sqrt{2}$

$\Delta S_3 = (\Delta C_2\text{–}H + \Delta C_5\text{–}H)/\sqrt{2}$

$\Delta S_4 = (\Delta C_3\text{–}H + \Delta C_4\text{–}H)/\sqrt{2}$

$\Delta S_5 = \Delta C_2\text{–}O\text{–}C_5$

$\Delta S_6 = (\Delta O\text{–}C_2\text{–}C_3 + \Delta O\text{–}C_5\text{–}C_4)/\sqrt{2}$

$\Delta S_7 = (\Delta O\text{–}C_2\text{–}H + \Delta O\text{–}C_5\text{–}H)/\sqrt{2}$

$\Delta S_8 = (\Delta C_2\text{–}C_3\text{–}H) + \Delta C_5\text{–}C_4\text{–}H)/\sqrt{2}$

0.01 are listed. Intensity of each vibrational level is classified into S (strong), M (medium) or W (weak) according to the magnitude of FCF. The present assignment is compared with the interpretation of the observed spectrum by Derrick et al. [3]. We note that they used the qualitative description of the vibration according to Lord and Miller [20]. We convert their notation in Table 6 according to Herzberg [19]. Comparing vibrational energies of the present calculation with that of Derrick et al., we overestimate from 8.3% to 14.5%. A magnitude of the overestimation is the same order as that of the ground state. The present interpretation of the observed vibrational energies of 839 and 1037 cm^{-1} is consistent with that by Derrick et al. They interpreted that the vibrational energies of 839 and 1037 cm^{-1} with strong intensity were the ν_8 and ν_6 transitions, respectively. The present assignment of 1944 cm^{-1} also consists of their assignment. It was assigned to the $\nu_6 + \nu_8$ transition. They interpreted that

Table 5. Classical half-amplitude of the zero-point vibrational levels

State	Component	ν_1	ν_2	ν_3	ν_4	ν_5	ν_6	ν_7	ν_8
$^1A_1$	$\Delta O{-}C_2$	−0.002	0.001	−0.016	−0.014	−0.008	0.031	0.012	0.005
	$\Delta C_2{-}C_3$	−0.006	−0.002	0.034	−0.015	−0.016	−0.004	0.002	0.002
	$\Delta C_2{-}H$	0.066	−0.029	0.003	−0.002	−0.001	0.002	−0.000	−0.001
	$\Delta C_3{-}H$	0.029	0.067	0.003	0.001	−0.003	0.001	−0.001	0.000
	$\Delta C_2{-}O{-}C_5$	−0.5	0.2	2.0	−0.2	0.4	−0.2	−0.9	−3.5
	$\Delta O{-}C_2{-}C_3$	0.3	−0.4	−0.7	1.4	−0.8	−0.4	−0.5	2.6
	$\Delta O{-}C_2{-}H$	−0.3	0.1	4.1	2.2	3.7	2.0	0.9	0.3
	$\Delta C_2{-}C_3{-}H$	0.1	−0.3	−0.3	4.6	−2.8	−0.8	3.6	−1.6
$^2A_2$	$\Delta O{-}C_2$	−0.002	0.002	−0.018	−0.014	−0.024	0.012	0.016	0.004
	$\Delta C_2{-}C_3$	−0.006	−0.001	0.004	0.031	−0.018	−0.025	0.004	0.004
	$\Delta C_2{-}H$	0.060	−0.040	0.001	0.002	−0.004	−0.000	0.001	−0.001
	$\Delta C_3{-}H$	0.040	0.060	0.004	−0.001	−0.003	−0.002	−0.001	0.001
	$\Delta C_2{-}O{-}C_5$	−0.4	0.3	0.9	1.9	−0.5	−0.5	−0.9	−3.5
	$\Delta O{-}C_2{-}C_3$	0.2	−0.4	0.8	−1.4	0.5	−0.3	−0.2	2.6
	$\Delta O{-}C_2{-}H$	−0.2	0.1	3.3	3.9	−0.1	3.7	0.9	0.2
	$\Delta C_2{-}C_3{-}H$	0.1	−0.3	3.5	−2.4	1.5	−1.7	4.3	−1.4
$^2B_1$	$\Delta O{-}C_2$	−0.003	0.001	−0.018	−0.014	−0.014	0.028	0.005	0.001
	$\Delta C_2{-}C_3$	−0.006	−0.003	0.032	−0.019	−0.018	−0.010	−0.001	0.005
	$\Delta C_2{-}H$	0.069	−0.020	0.002	−0.003	−0.002	0.002	−0.000	−0.001
	$\Delta C_3{-}H$	0.020	0.070	0.002	−0.000	−0.003	0.000	−0.002	0.000
	$\Delta C_2{-}O{-}C_5$	−0.5	0.1	2.3	−0.4	0.4	−0.7	−0.2	−3.6
	$\Delta O{-}C_2{-}C_3$	0.4	−0.3	−0.9	1.4	−0.5	−0.3	−1.0	2.5
	$\Delta O{-}C_2{-}H$	−0.3	0.0	4.8	2.0	2.0	3.0	0.9	0.3
	$\Delta C_2{-}C_3{-}H$	0.2	−0.3	−0.3	4.7	−3.7	−1.1	2.7	−1.2

Bond lengths are in angstroms, angles in degrees

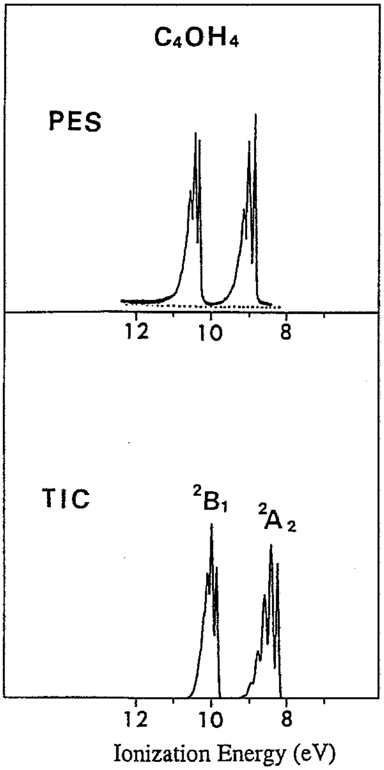

Fig. 2. The theoretical intensity curves of ionization of the $^2A_2$ and $^2B_1$ states with a half-width of 0.08 eV and the observed photoelectron spectrum by Turner et al. [2]. TIC: Theoretical intensity curve; PES: PE spectrum

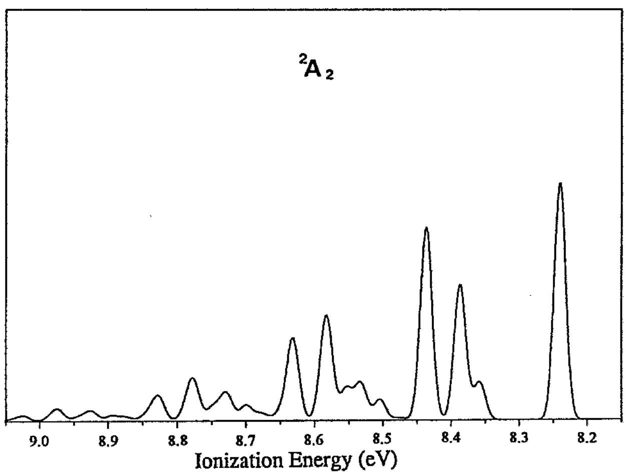

Fig. 3. The theoretical intensity curves of ionization of the $^2A_2$ sate with a half-width of 0.02 eV

the observed vibrational energy of 1420 cm^{-1} with strong intensity was the ν_3 mode, while the present calculation suggests to assign it as the ν_4 mode. They reported that the ν_3 mode also contributed to the vibrational energy of 2194, 2500 and 2823 cm^{-1}. The present calculation suggests that the ν_4 mode also contributes

Table 6. Assignment of the vibrational structure of the $^2A_2$ state

IE	Present calculation			Derrick et al.[a]		
	Vibrational energy (cm^{-1})	Intensity	Assignment	Vibrational energy (cm^{-1})	Intensity	Assignment
8.24	0	S	0	0	VS	0
8.36	953	M	ν_8	839	S	ν_8
8.38	1146	W	ν_7			
8.39	1187	S	ν_6	1037	S	ν_6
8.44	1578	S	ν_4	1420	S	ν_3
8.50	2140	W	$\nu_6 + \nu_8$	1944	W	$\nu_6 + \nu_8$
8.53	2374	W	$2\nu_6$	2194	M	$2\nu_6$
8.55	2531	W	$\nu_4 + \nu_8$			$\nu_3 + \nu_8$
8.58	2724	W	$\nu_4 + \nu_7$			
8.58	2765	M	$\nu_4 + \nu_6$	2500	M	$\nu_3 + \nu_6$
8.63	3156	M	$2\nu_4$	2323	M	$2\nu_3$
8.70	3718	W	$\nu_4 + \nu_6 + \nu_8$			
8.73	3952	W	$\nu_4 + 2\nu_6$			
8.75	4109	W	$2\nu_4 + \nu_8$			
8.78	4343	W	$2\nu_4 + \nu_6$			
8.83	4734	W	$3\nu_4$			

[a] Ref. [3]

IE: Ionization energy

Intensity of the present calculation is classified into S, M or W according to magnitude of FCF as follows: S: 0.22 > FCF > 0.10, M: 0.08 > FCF > 0.03 and W: 0.030 > FCF > 0.010

to these bands instead of the ν_3 mode. However, the character of the ν_4 mode of the $^2A_2$ state may correspond to that of the ν_3 mode of the ground state. Therefore, it should be said that the present interpretation of these band is consistent with that of Derrick et al. Table 6 indicates that the ν_7 mode contributes to the vibrational energies of 1037 and 2500 cm^{-1} even though with weak intensity.

The vibrational excitations of the ν_4 and ν_6 modes have large intensity in the $^2A_2$ state. This situation is connected to the change in the geometrical parameters by ionization. Table 1 reveals that the O–C_2 length becomes short (− 0.020 Å) and the C_2–C_3 length becomes long (+ 0.061 Å). Table 5 shows that a magnitude in the change of the C_2–C_3 length is larger than that of the classical half-amplitude of the zero-point vibrational level of each mode. The character of the ν_4 mode is a mixture of the O–C_2 and C_2–C_3 stretching motions coupled with out-of-phase mode. This phase is consistent with the phase of the change in the O–C_2 and C_2–C_3 lengths. The ν_6 mode is also a mixture of the O–C_2 and C_2–C_3 stretching motions couples with out-of-phase mode. Therefore, the higher vibrational excitation including the ν_4 and ν_6 modes mainly contribute to the intensity.

Table 7 shows an assignment of the vibrational structure of the $^2B_1$ state. The first band of the theoretical intensity curve is the zero–zero transition level. The second band with strong intensity is assigned to the ν_8 and ν_7 transitions. Derrick et al. have reported a PE spectrum which shows well-resolved vibrational structure. The second band of the PE spectrum is broader than the first band, while the present second band has more strong intensity compared to the first band (see Fig. 4). This situation should be connected to the underestimation of the separation

Table 7. Assignment of the vibrational structure of the $^2B_1$ state

	Present calculation			Derrick et al.[a]		
IE	Vibrational energy (cm^{-1})	Intensity	Assignment	Vibrational energy (cm^{-1})	Intensity	Assignment
9.87	0	S	0	0	VS	0
9.99	935	S	ν_8	871	S	ν_8
10.00	1026	M	ν_7	952	M	ν_7
10.02	1222	W	ν_5			
10.07	1589	M	ν_3	1355	W	ν_4
10.10	1870	M	$2\nu_8$	1855	M	$2\nu_8$
10.11	1961	M	$\nu_7 + \nu_8$			$\nu_7 + \nu_8$
10.12	2052	W	$2\nu_7$			$2\nu_7$
10.18	2524	M	$\nu_3 + \nu_8$	2799	W	$3\nu_7$
10.19	2615	W	$\nu_3 + \nu_7$			$2\nu_7 + \nu_8$
10.22	2805	W	$3\nu_8$			$3\nu_8$
10.23	2896	W	$\nu_7 + 2\nu_8$			$\nu_7 + 2\nu_8$
10.30	3459	W	$\nu_3 + 2\nu_8$			
10.31	3550	W	$\nu_3 + \nu_7 + \nu_8$			

[a] Ref. [3]
IE: Ionization energy
Intensity of the present calculation is classified into S, M or W according to magnitude of FCF as follows: S: 0.21 > FCF > 0.18, M: 0.08 > FCF > 0.05 and
W: 0.03 > FCF > 0.010

of the two vibrational energies between the ν_8 and ν_7 modes. The calculated value is 91 cm^{-1}. Derrick et al. have assigned the second band to the vibrational modes of ν_8 and ν_7. The vibrational energies of the ν_8 and ν_7 modes were 871 and 952 cm^{-1}, respectively. The separation of the two vibrational energies is 81 cm^{-1}. It is so small compared to the calculated value that the band should become sharper than the calculated one. By considering a broad feature of the band of the PE spectrum, we propose that it is necessary to reinterpret the observed vibrational energies of the ν_8 and ν_7 modes.

The observed vibrational energy of 1355 cm^{-1} was interpreted as the ν_4 mode. This energy should correspond to the present calculation of 1589 cm^{-1}, which is assigned to the ν_3 mode. The character of the ν_3 mode of the $^2B_1$ state corresponds to the ν_3 mode of the ground state. The observed vibrational energy of 1855 cm^{-1} was assigned to the $2\nu_8$, $\nu_7 + \nu_8$ and $2\nu_7$ modes. This assignment is consistent with the present result. The observed vibrational energy of 2799 cm^{-1} was assigned to the $3\nu_7$, $2\nu_7 + \nu_8$, $3\nu_8$ and $\nu_7 + 2\nu_8$ modes. This band should correspond to the calculated vibrational energy from 2524 to 2896 cm^{-1}. The FCFs of the $3\nu_8$ and $\nu_7 + 2\nu_8$ transitions are larger than 0.01, while those of the $3\nu_7$, $2\nu_7 + \nu_8$ transition are smaller than 0.01. The present calculation reveals that the $\nu_3 + \nu_8$ and $\nu_3 + \nu_7$ transitions contribute to the intensity.

The vibrational excitations of the ν_8, ν_7 and ν_3 modes contribute to the intensity in the $^2B_1$ state. This feature is ascribed to the change in the geometrical parameters by ionization. Table 1 shows that the C_2–O–C_5 angle of the $^2B_1$ state becomes wide by 6.6°. A magnitude of the change is larger than that of the classical half-amplitude of the zero-point vibrational level of each mode. It is also found

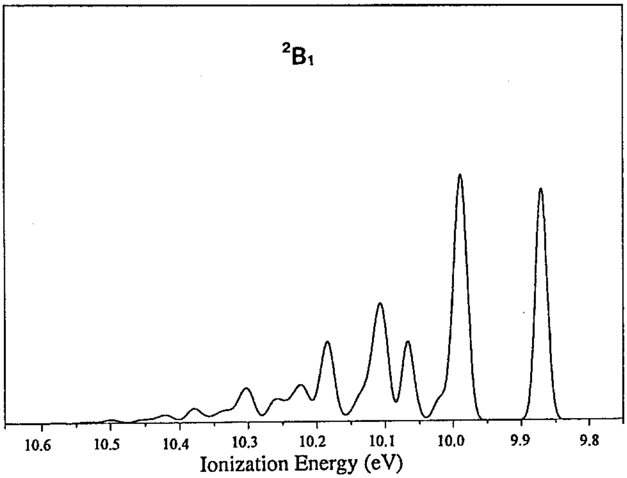

Fig. 4. The theoretical intensity curves of ionization of the $^2B_1$ state with a half-width of 0.02 eV

from Table 1 that the O–C_2 length becomes short, the C_2–C_3 length becomes long, the O–C_2–C_3 bond angle becomes narrow and the O–C_2–H and C_2–C_3–H angles become wide. The ν_8 mode has a large amplitude in the C_2–O–C_5, O–C_2–C_3 and C_2–C_3–H bending motions and the phase of these bending motions is consistent with the change in the geometry by ionization. Thus, vibrational transition of ν_8 mode has strong intensity. The ν_7 mode has an amplitude in the O–C_2–C_3, O–C_2–H and C_2–C_3–H bending motions. The ν_3 mode has an amplitude in the O–C_2 and C_2–C_3 stretching motions, C_2–O–C_5 and O–C_2–H bending motions. The phases of these vibrational motions are also consistent with the change in the geometry by ionization. Therefore, the ν_7 and ν_3 modes contribute to the intensity.

4. Conclusion

The molecular equilibrium structures and vibrational frequencies are calculated for the ground and lower two ionic states. By the use of the FCFs, we obtain the theoretical intensity curve of the $^2A_2$ and $^2B_1$ states. The theoretical intensity curves are in good agreement with the observed PE spectra.

Derrick et al. interpreted the vibrational structure of the $^2A_2$ state by using the ν_8, ν_6 and ν_3 modes. The present calculation reveals that the ν_8, ν_6, ν_7 and ν_4 modes contribute to the intensity. The present notation of each mode is arranged in order of a magnitude of the frequency. The character of the ν_4 mode of the $^2A_2$ state may correspond to that of the ν_3 mode of the ground state. The character of the ν_7 and ν_8 modes should correspond to those of the ground state. The vibrational transitions of the ν_6 and ν_4 modes have large intensity. This situation is connected to the change in the geometrical parameters by ionization where the O–C_2 length becomes short and the C_2–C_3 length becomes long. Both ν_6 and ν_4 modes have an amplitude in the O–C_2 and C_2–C_3 stretching motions and the phase of motion is consistent with the change in the geometry by ionization. The contribution of the ν_7 mode to the intensity is weak.

Derrick et al. interpreted the vibrational structure of the $^2B_1$ state by using the ν_8, ν_7 and ν_4 modes. The present calculation shows that the ν_8, ν_7 and ν_3 modes contribute to the intensity and the character of each mode corresponds to that of the ground state. The present assignment of the lower five bands is consistent with that of Derrick et al. except for the contribution of the ν_4 mode. The ν_3 mode contributes to the intensity instead of the ν_4 mode. The ν_8 and ν_7 transitions contribute to the second band. The separation of the vibrational energies between the ν_8 and ν_7 modes were reported as 81 cm^{-1}. Considering the broad feature of the second band, we propose that the separation should be more large. The sixth band with frequency of 2799 cm^{-1} was interpreted as the $3\nu_7$, $2\nu_7 + \nu_8$, $3\nu_8$ and $\nu_7 + 2\nu_8$ modes. The FCFs of the $3\nu_8$ and $\nu_7 + 2\nu_8$ transitions are larger than 0.01, while those of the $3\nu_7$, $2\nu_7 + \nu_8$ transitions are smaller than 0.01. The present calculation of FCF reveals that the $\nu_3 + \nu_8$ and $\nu_3 + \nu_7$ transitions should contribute to the intensity. The contributions of the ν_8, ν_7 and ν_3 modes to the intensity should be connected the change in the geometrical parameters by ionization. The O–C_2 length becomes short, the C_2–C_3 length becomes long, the O–C_2–C_3 bond angle becomes narrow and the C_2–O–C_5, O–C_2–H and C_2–C_3–H angles become wide. The ν_8 mode has large amplitude in the C_2–O–C_5, O–C_2–C_3 and C_2–C_3–H bending motions. The ν_7 mode has an amplitude in the O–C_2–C_3, O–C_2–H and C_2–C_3–H bending motions. The ν_3 mode has an amplitude in the O–C_2 and C_2–C_3 stretching motions. C_2–O–C_5 and O–C_2–H bending motions. The phases of these vibrational motions are consistent with the change in the geometry by ionization. Therefore, the ν_8, ν_7 and ν_3 modes contribute to intensity.

Acknowledgement. Computation was carried out on HITAC M-680H systems at the Center for Information Processing Education of Hokkaido University.

References

1. Baker AD, Betteride D, Kemp NR, Kirby RE (1970) Anal Chem 42:1064
2. Turner DW, Baker AD, Baker C, Brundle CR (1970) Molecular photoelectron spectroscopy. Wiley–Interscience, London
3. Derrick PJ, Åsbrink L, Edqvist O, Lindholm E (1971) Spectrochimica Acta 27A: 2525
4. Sell JA, Kuppermann A (1979) Chem Phys Lett 15:355
5. Munakata T, Kuchitu K, Harada Y (1980) J Electron Spectrosc Relat Phenom 20:235
6. Kimura K, Katsumata S, Achiba Y, Yamazaki T, Iwata S (1981) Handbook of HeI photoelectron spectra of fundamental organic molecules. Halsted, New York
7. Klasinc L, Sabljic A, Kluge G, Rieger J, Scholz M (1982) J Chem Soc Perkin Trans II:539
8. von Niessen W, Cederbaum LS, Diercksen GHF (1976) J Am Chem Soc 98:2066
9. Dealti G, Decleva P, Lisini A (1984) Chem Phys 90:231
10. Nakatsuji H, Kitao O, Yonezawa T (1985) J Chem Phys 83:723
11. Cordell FR, Boggs JE (1981) J Mol Struct 85:163
12. Tatewaki H, Huzinaga S (1980) J Comput Chem 1:205
13. Mclean AD, Liu B (1973) J Chem Phys 58:1066
14. Shoda T, Noro T, Nomura T, Ohno K (1986) Int J Quantum Chem 30:289
15. Takeshita K (1987) J Chem Phys 86:329
16. Takeshita K, Sasaki F (1979) 1981 Library program at the Hokkaido University Computing Center (in Japanese). GRAMOL included the Program JAMOL3 of the RHF calculation written by Kashiwagi H, Takada T, Miyoshi E, Obara S for the Library program at the Hokkaido University Computing Center (in Japanese)
17. Murakami A, Iwaki H, Terashima H, Shoda T, Kawaguchi T, Noro T 1986 Library program at the Hokkaido University Computing Center (in Japanese)
18. Nygaard L, Nielsen JT, Kirchheiner J, Maltesen G, Rastrup-Andersen J, Soreensen GO (1969) J Mol Struct 3:491
19. Herzberg G (1966) Molecular spectra and molecular structure. Part III. van Nostrand, New York
20. Loard RC, Miller FA (1942) J Chem Phys 10:328